Isothermal Kinetic Measurements for the Hydrogenation of Ethylene on Pt(111) under Vacuum: Significance of Weakly-Bound Species in the Reaction Mechanism

Helmut Öfner and Francisco Zaera*

Department of Chemistry, University of California, Riverside, California 92521

Received: October 3, 1996; In Final Form: November 11, 1996[⊗]

The kinetics of the hydrogenation of ethylene on Pt(111) was studied isothermally and under vacuum by using a variation of the dynamic molecular beam method originally devised by King and Wells. At surface temperatures above 240 K ethylidyne formation competes with both ethylene hydrogenation and ethylene desorption. At temperatures below 240 K, on the other hand, the decomposition of ethylene is slow, and the adsorption and hydrogenation kinetics for ethylene on both clean and hydrogen-covered surfaces could be investigated independently. Ethylene adsorption was found to be precursor-mediated at low coverages and Langmuirian near saturation. A certain population of weakly-adsorbed species can also be maintained at coverages near saturation by exposure of the surface to a constant flux of ethylene molecules. The presence of coadsorbed hydrogen reduces the total ethylene uptake but increases the amount of weakly-adsorbed ethylene as compared to that on the clean Pt(111). The main conclusion from this work is the fact that this weakly-adsorbed species appears to be essential for the hydrogenation of ethylene: the kinetic orders of the reaction were determined to be 1.2 ± 0.3 and 0.8 ± 0.2 with respect to the weakly-adsorbed ethylene and hydrogen surface coverages, respectively. An activation energy of 6 ± 1 kcal/mol was measured for the hydrogenation of ethylene to ethane under the conditions of these experiments. Finally, the presence of ethylidyne on the surface was found to not influence the hydrogenation reaction in any other way than by blocking surface sites.

1. Introduction

Since its discovery at the end of the 19th century, the hydrogenation of olefins over metal catalysts has been one of the most thoroughly studied chemical processes.[1,2] In order to develop a picture for the mechanism of this reaction at the molecular level, much effort has been put into the understanding of the reaction of the smallest olefin, C_2H_4, on late transition metals and in particular on the Pt(111) surface. These studies have revealed at least two reaction regimes:[3] (1) That under catalytic conditions, at C_2H_4 and H_2 pressures above the milliTorr range, and around or above room temperature. Under those conditions the hydrogenation of ethylene occurs in the presence of an ethylidyne ($Pt_3{\equiv}CCH_3$) layer that covers the Pt catalyst.[4−6] (2) That under ultrahigh-vacuum (UHV) conditions, which has usually been studied on single-crystal surfaces and which involves submonolayer coverages of C_2H_4 and H_2. According to results from temperature-programmed desorption (TPD) work, hydrogenation in the latter case occurs directly on the clean substrate.[7,8] However, since several competing reactions occur simultaneously on Pt(111) surfaces covered with coadsorbed C_2H_4 and H between 250 and 300 K (i.e., H_2 and C_2H_4 desorption, conversion of C_2H_4 to ethylidyne, and hydrogenation of C_2H_4 to ethane), the inherent problems of TPD, namely, the fact that both surface temperature and surface coverages change simultaneously during the experiment, make a clear analysis of the kinetics of these reactions extremely difficult. Such problems can be minimized by employing dynamic isothermal methods such as that originally devised by King and Wells.[9]

This paper presents results from experiments performed by using a variation of the King and Wells approach[10,11] on surfaces with well-defined coverages of both ethylene and hydrogen. It was found that ethylene adsorption goes through an initial precursor-mediated stage which is followed by a Langmuir-type behavior close to saturation. The molecules in the latter phase are weakly adsorbed (probably π bonded) and desorb reversibly under vacuum, but a steady-state population of such species builds up on the surface in the presence of a continuous flux of ethylene molecules from the gas phase. The key observation from this work is the fact that the reported data points to the particular importance of this weakly-adsorbed ethylene in the hydrogenation of ethylene to ethane: there is a nearly first-order dependence (1.2 ± 0.3) of the rate of ethylene hydrogenation on the coverage of the weakly-adsorbed ethylene. The hydrogenation reaction also displays a near to first-order dependence (0.8 ± 0.2) on the concentration of surface hydrogen and an activation energy of 6 ± 1 kcal/mol. A comparison of the kinetic study under vacuum described below with previous work under catalytic conditions suggests that the limiting step in the latter case is the competitive adsorption of hydrogen in the presence of ethylene. Finally, the role of ethylidyne seems to be only to block adsorption sites.

2. Experimental Section

All the experiments reported here were performed in a 6.0 L stainless steel ultrahigh-vacuum (UHV) chamber evacuated with a 300 L/s turbomolecular pump to a base pressure of about 5×10^{-10} Torr and equipped with a UTI 100C quadrupole mass spectrometer, a sputtering ion gun, and a molecular beam doser. A detailed description of the doser setup and of its calibration has been given elsewhere.[10] Briefly, the doser, which consists of a 1.2 cm diameter array of parallel microcapillary glass tubes, is connected to a calibrated volume via a leak valve and a second shut-off valve that isolates it from the main vacuum vessel. The beam flux is set by filling the backing volume to a specific pressure, which is measured by a MKS baratron gauge, and by adjusting the leak valve to a predetermined set point. A movable stainless steel flag is placed between the sample and the doser

[⊗] Abstract published in *Advance ACS Abstracts,* January 1, 1997.

S1089-5647(96)03030-1 CCC: $14.00

in order to intercept the beam at will. The sample, a 0.9 cm diameter Pt(111) single crystal, is cleaned by a combination of Ar^+ ion sputtering, oxygen exposures at 800 K, and annealing to 1100 K before each experiment and is placed at a distance of 0.75 cm from the front of the doser to assure a reasonably flat gas flux profile.[10] The normal (99.5% purity, Matheson) and deuterated (99 atom % D, Cambridge Isotope Laboratories) ethylenes were used as supplied, and the hydrogen (99.999%, Matheson) was purified with an in-line liquid nitrogen trap.

The time evolution of the partial pressures of up to 10 different species was followed in both the isothermal kinetics and the temperature-programmed desorption (TPD) experiments by using the quadrupole mass spectrometer, which was placed out of the line of sight of the beam and the crystal in order to avoid any artifacts due to possible angular dependencies of either the scattering or the desorption of the gases and which was interfaced to a personal computer. The mass spectrometer signal for ethylene was calibrated by equating the time-integrated ethylene uptake on clean Pt(111) below 200 K to the saturation coverage of ethylene on Pt(111), which was assumed to be 0.25 monolayers (ML).[12−14] The ethane signal was then calibrated by using the relative mass spectrometer sensitivities for ethane and ethylene,[15] and the hydrogen flux was calibrated relative to that of ethylene by taking into account the differences in effusion rates between the two gases in the doser, measured by following the decay of the pressures for each of the gases in the back volume over time. The platinum sample was heated resistively and cooled by using a liquid nitrogen reservoir, and its temperature was measured by a chromel−alumel thermocouple spot-welded to the back of the sample. TPD spectra were recorded at a heating rate of about 15 K/s.

3. Results

3.1. General Experimental Procedure. The experimental procedure for the isothermal kinetic measurements discussed in this paper is illustrated by the data in Figure 1, which shows typical uptake spectra (partial pressures versus time) for ethylene on Pt(111) at a sample temperature of 270 K. The signals for 2, 25, and 30 amu, representative of hydrogen, ethylene, and ethane, respectively, were monitored in this case. The adsorption of ethylene in particular can be studied by following the time evolution of the signal for ethylene (25 amu): (1) At $t = -t_1$, the shut-off valve is opened, and the ethylene gas, which is already set to a predetermined pressure in the backing volume, is let to enter the UHV chamber via the leak valve (also preset to a specific leak rate) and the doser. At this point the pressure of ethylene in the chamber raises to a new steady-state value because of the molecules that scatter into the vacuum after hitting the intercepting flag. (2) At $t = 0$ s the flag is then removed to allow for the ethylene beam to impinge directly on the surface. This results in a drop in ethylene partial pressure due to its adsorption on the Pt(111) surface, which is visible as a dip in the 25 amu trace in Figure 1 and which is proportional to the ethylene sticking probability (see below). (3) The ethylene uptake continues until the surface becomes saturated, at which point its partial pressure returns to the value reached before the removal of the flag. (4) At $t = t_2$ the flag is placed in front of the surface again, causing a brief increase in the ethylene partial pressure because of the desorption of some weakly-adsorbed ethylene which takes place immediately after blocking of the beam. (5) At $t = t_3$ the flag is removed again, leading to the reverse process, namely, to a sharp drop in the ethylene partial pressure due to the uptake of some additional ethylene on the surface. (6) The behavior seen at $t = t_2$ and $t = t_3$ is reversible and can be repeated indefinitely. (It was done three more times in this experiment.) (7) Finally, the doser is turned off, in this case at approximately $t = 110$ s, and all partial pressures are let to return to their background levels.

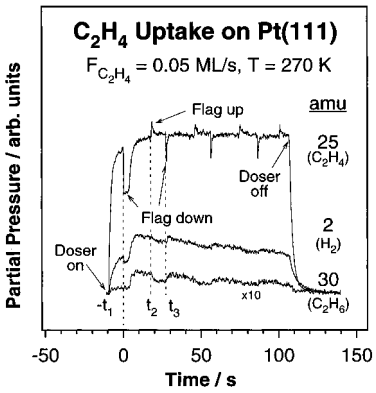

Figure 1. Typical isothermal kinetic curves obtained with the experimental setup described in the text for the uptake of ethylene on Pt(111) at 270 K. The time evolution of the mass spectrometry signals for ethylene (25 amu), hydrogen (2 amu), and ethane (30 amu) is used to follow the three different reactions that compete on the surface under these conditions, namely, ethylene adsorption−desorption, ethylidyne formation, and hydrogenation of ethylene to ethane, respectively. The effusive collimated ethylene beam was set at a flux of 0.05 ML/s.

Besides ethylene adsorption−desorption, two more reactions can be followed in these experiments, namely, the decomposition of ethylene to ethylidyne ($Pt_3{\equiv}CCH_3$) and the hydrogenation of ethylene to ethane. The former produces one H atom per ethylene molecule and therefore becomes evident by an increase in the partial pressure of hydrogen. Indeed, although the hydrogen signal (the 2 amu trace) in Figure 1 decreases suddenly at $t = 0$ s (following the 25 amu trace because of the contribution from the cracking of ethylene in the mass spectrometer to its intensity), it does increase at later times above the background level as a result of the formation of ethylidyne. This effect becomes more noticeable at higher temperatures and can be used to follow the kinetics of ethylidyne formation (see below). The self-hydrogenation of ethylene to ethane can be detected by the changes in signal intensity in the 30 amu trace. The nonzero background intensity of this signal before $t = 0$ s is due to a small amount of ethane contamination in the ethylene beam, but the steep increase above that level once the ethylene coverage approaches saturation clearly originates from the evolution of ethane from the surface; the intensity of the 30 amu signal also drops significantly during the periods when the ethylene beam is blocked by the flag (for instance, during $t_2 < t < t_3$).

The interplay of the three reactions discussed in this paragraph, i.e., the dynamic ethylene adsorption−desorption equilibrium, the formation of ethylidyne, and the hydrogenation of ethylene to ethane, will be addressed individually in more detail in the following sections.

3.2. Formation of Ethylidyne and Self-Hydrogenation of Ethylene. The formation of ethylidyne and the self-hydrogenation of ethylene to ethane were followed independently in our isothermal kinetic experiments. Figure 2 displays the time evolution of the hydrogen (2 amu) signal during the exposure of clean Pt(111) to a constant ethylene beam at different temperatures. As mentioned above, two main contributions to the signal can be clearly identified in the spectra, one due to the cracking of ethylene and another from H_2 evolution during the conversion of ethylene to ethylidyne, but the first can be estimated by

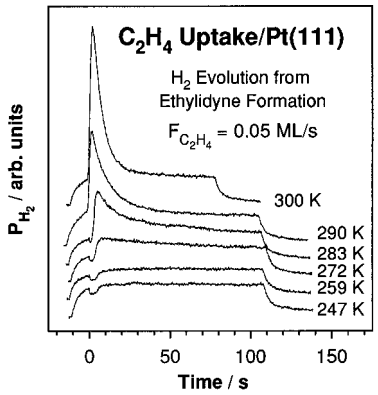

Figure 2. Time evolution of the partial pressure of hydrogen during the exposure of a Pt(111) crystal to an ethylene beam of 0.05 ML/s flux as a function of surface temperature.

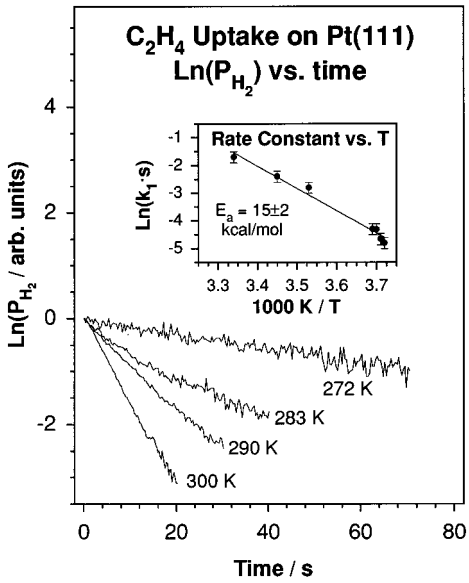

Figure 3. Main frame: time evolution of the hydrogen partial pressure during the uptake of ethylene on Pt(111) at different surface temperatures, the same as in Figure 2, but plotted on a logarithmic scale. Inset: Arrhenius plot of the reaction rate constants for ethylidyne formation (k_1), calculated from the temporal decay of the hydrogen partial pressure (as explained in the text), as a function of temperature.

comparison with the time evolution of other traces associated with C_2H_4 (e.g., 25, 26, 27, and 28 amu) and eliminated from the raw data. In any case, it is clear that the H_2 signal intensity does increase above the level associated with the cracking of ethylene, even though this occurs only after completion of the ethylene adsorption process (especially at low temperatures). The contribution from ethylidyne formation to the H_2 signal becomes more prominent at higher temperatures and is the dominating component at $T > 280$ K.

Figure 3 displays some of the data from Figure 2 but on a logarithmic scale and after subtraction of the contribution from the cracking of ethylene. The *y* axis of the spectra has also been shifted in this plot to a common starting point at $t = 0$ s (which was redefined as the beginning of the desorption of H_2) for display purposes. The approximately linear behavior seen in these curves implies an exponential decay of the H_2 signal with time indicative of a first-order behavior. Also, the initial slope of these traces was used to estimate the reaction rate constants (k_1) for ethylidyne formation at the different temperatures, and those were then plotted in an Arrhenius fashion in the insert of Figure 3. An activation energy E_a of about 15 ± 2 kcal/mol was obtained for the formation of ethylidyne this way, in agreement with published work.[16−19]

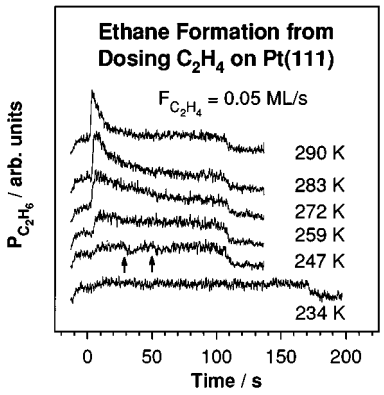

Figure 4. Ethane partial pressure as a function of time for a Pt(111) surface exposed to a constant ethylene beam at different surface temperatures ($F_{C_2H_4} = 0.05$ ML/s). The arrows below the 247 K trace mark the points in time when the ethylene beam to the surface was intercepted by raising the blocking flag.

Figure 4 displays the time evolution of the ethane (30 amu) that results from the hydrogenation of surface ethylene under the same experimental conditions as in Figure 2. That signal jumps above the background level upon exposing the surface to the beam ($t > 0$ s), after which it reaches a maximum and then decays slowly in time. Also, the drop in signal intensity during the blocking of the beam, which was done at the points marked by the arrows below the 247 K trace, proves that indeed the rate of ethane formation correlates with the reduction in ethylene pressure in front of the surface (see also Figure 1). Note that the 30 amu signal does remain above the background level even when the beam is blocked, most likely because that blocking does not completely suppress ethylene adsorption from the background; from the flux dependence of the hydrogenation rate and the drop in the hydrogenation rate after beam blocking, this background contribution is estimated to be about one-eighth of that from the direct beam (see below). Overall, the temporal evolution of the ethane signal at the different temperatures resembles the behavior seen in Figure 2 for H_2: in the case of the 283 K trace, for instance, the ratio $R_{ethylidyne}/R_{ethane}$ remains at a constant value of about 10 until all the ethylene adsorbed on the surface is converted to ethylidyne. The data from Figure 4 were also used to estimate the total amount of ethane produced (by integration of the signal), which equals approximately 0.025 ML for the 283 K trace or about 10% of the ethylene molecules in a saturated ethylene layer.

3.3. Ethylene Adsorption on Clean and Hydrogen-Precovered Pt(111) Surfaces. It is clear from the results presented so far that above 240 K the chemistry of ethylene on Pt(111) is quite complex, because it involves three simultaneous and competing reactions, namely, ethylene adsorption−desorption, ethylidyne formation, and ethane formation. In order to investigate the mechanism for the hydrogenation of ethylene to ethane while avoiding the complications arising from the concurrent reactions (the formation of ethylidyne and the ethylene self-hydrogenation triggered by the release of hydrogen atoms on the surface), the experiments in the following section were performed at temperatures below 240 K.

3.3.1. Adsorption on Clean Pt(111). The adsorption kinetics for ethylene on clean Pt(111) will be addressed first. Figure 5a displays an example of a C_2H_4 uptake curve on clean Pt(111) at $T = 190$ K. As explained before, the pressure drop $\Delta P(t)$ that starts at $t = 0$ s is induced by the removal of the flag from the path of the beam and reflects the adsorption of C_2H_4 on the Pt(111) surface. The dashed line is a combination of an exponential and a linear function to represent the C_2H_4 equilibrium pressure ($P_{eq}(t)$) expected if the beam were to remain

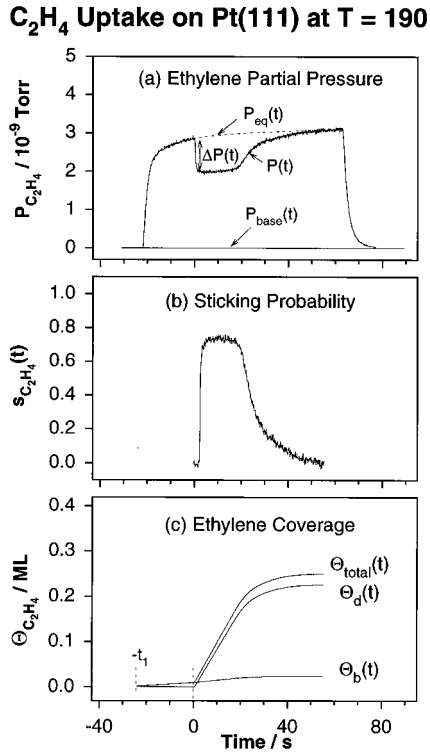

Figure 5. (a, top) Time evolution of the partial pressure of ethylene during dosing of a Pt(111) surface with a collimated C_2H_4 beam at 190 K. The surface exposure starts at $t = 0$ s. (b, center) Ethylene sticking probability versus time calculated from (a). (c, bottom) Time evolution of the total ethylene coverage ($\Theta_{total}(t)$) and of the contributions due to the direct beam ($\Theta_d(t)$) and to background adsorption ($\Theta_b(t)$), also calculated from (a).

blocked during that time. The sticking coefficient for ethylene, $s_{C_2H_4}(t)$, can be evaluated by using the data in both traces and by following the formalism of Madey:[20]

$$s_{C_2H_4}(t) = \frac{1}{f}\frac{\Delta P(t)}{P_{eq}(t) - P_{base}(t)} = \frac{1}{f}\frac{P_{eq}(t) - P(t)}{P_{eq}(t) - P_{base}(t)} \quad (1)$$

where f, the fraction of the beam intercepted by the crystal, has been experimentally determined to be 0.425 in our setup.[10] Figure 5b displays the result of applying eq 1 to the data of Figure 5a and shows that the sticking coefficient of ethylene on the clean surface remains constant at about 0.7 for most of the uptake, indicating precursor-mediated adsorption.[21]

The time evolution of the coverage of ethylene on the surface during adsorption can be estimated from the data as well. For this, the contributions from the direct beam and the background need to be considered separately. The coverage increase arising from adsorption of molecules from the background, $\Theta_b(t)$, is given by[10]

$$\Theta_b(t) = \frac{\beta}{A}\int_{-\infty}^{t} s_{C_2H_4}(\tau)\, P(\tau)\, d\tau \approx \frac{\beta}{A}\, s^{\circ}_{C_2H_4}\int_{-\infty}^{0} P(\tau)\, d\tau + \frac{\beta}{A}\int_{0}^{t} s_{C_2H_4}(\tau)\, P(\tau)\, d\tau \quad (2)$$

where the first term accounts for adsorption before the flag is removed, $t < 0$ s (in practice, the integral is only relevant from $t = -t_1$, the time when the ethylene beam is switched on); since during this time interval the sticking coefficient $s_{C_2H_4}(t)$ cannot be determined from the data, it is considered to be approximately constant at a value $s^{\circ}_{C_2H_4}$ equal to the average of the $s_{C_2H_4}(t)$ measured during the first 10 s after exposure of the surface to the direct beam. The proportionality constant β was estimated by using a gas temperature of 300 K, and the sample surface area A was measured to be 0.64 cm^2.

The term corresponding to the ethylene coverage buildup due to the exposure of the sample to the direct beam, $\Theta_d(t)$, can be expressed as

$$\Theta_d(t) = \frac{\alpha}{A}\int_0^t \Delta P(\tau)\, d\tau \quad (3)$$

where α is a constant whose value was determined by assuming that the sum $\Theta_{total}(t) = \Theta_d(t) + \Theta_b(t)$ at the end of the uptake on the clean surface is 0.25 ML. The time evolutiond of $\Theta_b(t)$, $\Theta_d(t)$, and $\Theta_{total}(t)$ calculated with eqs 2 and 3 are all displayed in Figure 5c. The ratio between the contributions for adsorption from the background and the direct beam was estimated from these calculations to be about 1:10, but this must be taken as a lower limit, since the density of gas-phase ethylene near the doser is higher in our experimental setup than at the position of the ion gauge used to estimate the background pressure. Comparing the rate of ethane formation for two extreme cases, during direct exposure to the beam and during background exposure in an experiment where the beam was blocked throughout the whole run, led to a value of about 1:8.

3.3.2. Adsorption on H_2-Predosed Pt(111). Plots of $s_{C_2H_4}$ versus Θ for the uptake of ethylene can be constructed by combining data such as those in Figure 5b,c. Examples of this are given in Figure 6a, a figure that also addresses the changes in the C_2H_4 uptake induced by hydrogen coadsorption, as studied by dosing the surface with a predetermined amount of hydrogen prior to exposure to the ethylene beam. The hydrogen precoverage in the example in Figure 6a was estimated to be about $\Theta_H = 0.5 \pm 0.2$ ML both by comparing our hydrogen TPD results (desorption maxima as a function of coverage) with literature results[22] and by calibrating the amount of H_2 that desorbs in those experiments to the yield obtained by decomposing a saturated ethylidyne layer (assuming an ethylidyne saturation coverage on Pt(111) of 0.25 ML). The sticking coefficients for ethylene on both clean and H-precovered surfaces show a qualitatively similar behavior; namely, they start high (about 0.7) and stay constant for most of the uptake but decrease linearly to zero when approaching saturation. This indicates that the type of adsorption changes from non-Langmuirian (precursor-mediated) to Langmuirian once a certain threshold coverage is reached. The presence of surface hydrogen does induce a reduction in both the saturation coverage and the coverage necessary for this change in the type of adsorption and, in addition, slightly reduces the value of the initial ethylene sticking coefficient. The first effect is illustrated more clearly for a sample temperature of 230 K in Figure 6b, which shows a linear decrease in the saturation coverage of ethylene with the amount of hydrogen present on the surface, by up to about 70%. This behavior can be explained by a competition for surface sites between the two species.

Figure 7 shows the effect that blocking (up arrow) and unblocking (down arrow) the ethylene beam impinging on clean and hydrogen-predosed Pt(111) surfaces has on the evolution of the ethylene partial pressure once ethylene saturation has been reached. These data show that intercepting the ethylene flux leads to the desorption of C_2H_4 in both cases, indicating that there is some weakly-bound ethylene present on the surface during the C_2H_4 exposure, as mentioned above. Also, exposing the depopulated surface back to the ethylene beam results in an adsorption dip in the ethylene signal, reflecting the repopulation of that weakly-bound state once the effective C_2H_4 pressure is increased again. The existence of a second, weaker adsorption state for ethylene at high coverages has already been

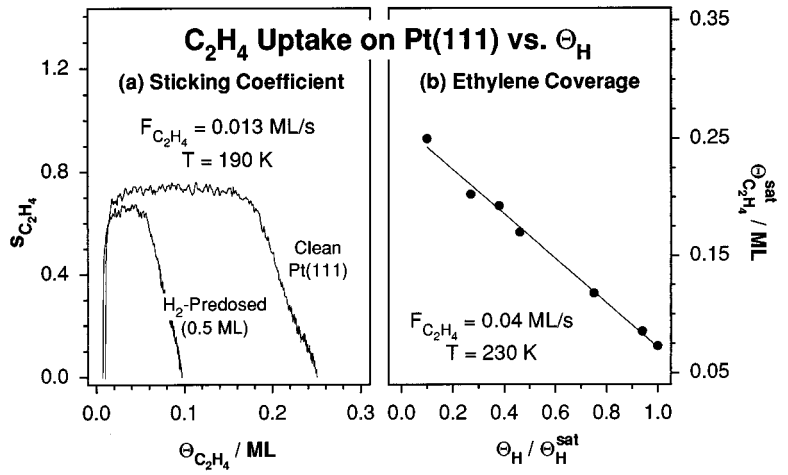

Figure 6. (a, left) Ethylene sticking coefficient as a function of ethylene coverage on clean and hydrogen-precovered ($\Theta_H = 0.5$ ML) Pt(111) surfaces at 190 K. (b, right) Total ethylene uptake on hydrogen-precovered Pt(111) surfaces at 230 K as a function of H coverage.

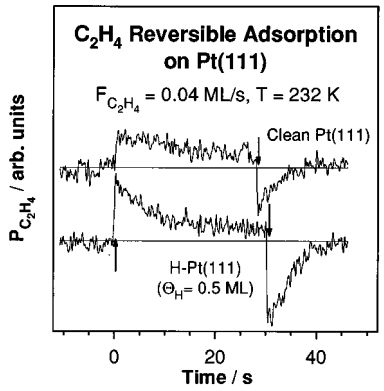

Figure 7. Ethylene partial pressure as a function of time for clean and hydrogen-predosed ($\Theta_H = 0.5$ ML) Pt(111) surfaces exposed to a constant ethylene beam ($F_{C_2H_4} = 0.04$ ML/s) at $T = 232$ K after reaching surface saturation. The ethylene beam to the surface was blocked at $t = 0$ s (up arrow), and the surface was exposed to the beam again at approximately $t = 30$ s (down arrows).

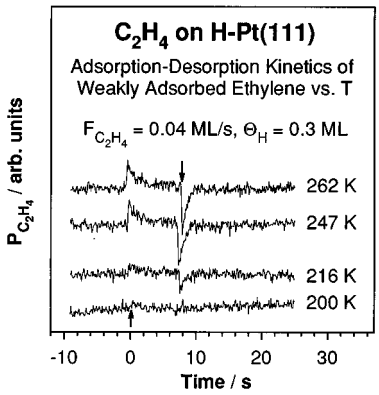

Figure 8. Ethylene partial pressure versus time for a hydrogen-predosed ($\Theta_H = 0.5$ ML) Pt(111) surface exposed to a constant ethylene beam ($F_{C_2H_4} = 0.04$ ML/s) at different surface temperatures after reaching ethylene saturation. As in Figure 7, the beam was blocked at $t = 0$ s (up arrow) and unblocked again at $t = 8$ s (down arrow).

observed in TPD experiments,[7] and the coexistence of strongly-bound di-σ and weakly-bound π ethylene on Pt(111) surfaces in the presence of high ethylene pressures has been characterized by infrared (IR) and sum-frequency generation (SFG) investigations.[23,24] Note, however, that even though the clean and H-precovered surfaces show a qualitatively similar behavior during the ethylene uptake, the number of desorbing ethylene molecules once the beam is blocked is about a factor of 2 higher from the H-precovered surface.

The temperature dependence of the equilibrium coverage of this weakly-bound ethylene was studied next. Adsorption−desorption traces such as those in Figure 7 are displayed in Figure 8 for hydrogen-presaturated surfaces exposed to a constant C_2H_4 flux of 0.04 ML/s at different temperatures. It is seen there that the initial desorption rate measured experimentally stays approximately constant when rising the surface temperature from 247 to 262 K, most likely because a close-to-temperature-independent equilibrium is reached almost immediately after exposure of the surface to the beam due to the fast rates of both the adsorption and the desorption of ethylene. Decreasing the surface temperature below 240 K, on the other hand, strongly reduces the size of the initial signal intensity jump, indicating that the desorption rate of the weakly-adsorbed ethylene dominates the overall kinetics in this regime; this weakly-bound state is in fact quite stable on the surface below 200 K.

In order to probe the amount of weakly-adsorbed ethylene that builds up on the surface as a function of ethylene flux, a hydrogen-predosed ($\Theta_H = 0.5$ ML) Pt(111) surface was exposed to ethylene beams of various fluxes at $T = 227$ K. The beam was intercepted with the flag after reaching the saturation coverage, and time evolution traces for the desorbing ethylene like those in Figure 8 were recorded. Since blocking the beam does not completely stop ethylene adsorption from the background but only reduces the ethylene flux to the surface by about a factor of $^1/_8$ (see above), the final coverage of weakly-adsorbed ethylene reached at a particular flux F_1 was determined by integrating the signal from the desorbing ethylene after blocking the direct beam over time and then adding the amount estimated in the same way when exposing the surface to a direct beam with a flux $F_2 = {}^1/_8 F_1$. Figure 9 displays the resulting weakly-adsorbed ethylene coverage $\Theta^{weak}_{C_2H_4}$ as a function of ethylene flux ($F_{C_2H_4}$). It appears from this figure that the adsorption−desorption kinetics of the weakly-bound ethylene is well described by a simple Langmuir model, as also indicated by the fact that at the high ethylene coverages needed to populate the weakly-bound state the sticking coefficient $s_{C_2H_4}(\Theta)$ decreases linearly with coverage (Figure 6a). According to the Langmuir hypothesis

$$\frac{d\Theta^{weak}_{C_2H_4}}{dt} = F_{C_2H_4} S_{C_2H_4}\left[1 - \frac{\Theta^{weak}_{C_2H_4}}{Q^{weak,max}_{C_2H_4}}\right] - k_d \Theta^{weak}_{C_2H_4} \qquad (4)$$

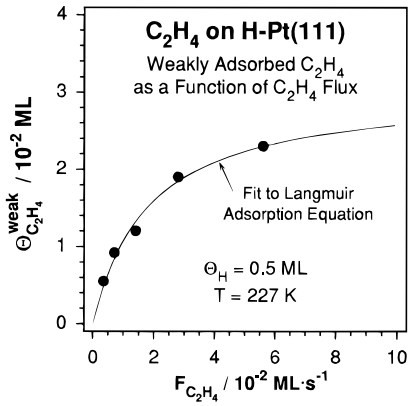

Figure 9. Coverage of weakly-adsorbed ethylene ($\Theta_{C_2H_4}^{weak}$) as a function of ethylene flux ($F_{C_2H_4}$) during dosing of a hydrogen-predosed (Θ_H = 0.5 ML) Pt(111) surface with ethylene at 227 K. The experimental data were fit to a Langmuir equation, as explained in the text.

where k_d is the desorption rate constant for the weakly-adsorbed ethylene and $S_{C_2H_4}$ is the intrinsic sticking coefficient of C_2H_4 at these high coverages. The equilibrium coverage for the weakly-bound ethylene can then be calculated from eq 4 for a particular value of $F_{C_2H_4}$ by assuming steady-state conditions, that is, by setting the overall rate to zero. The result is

$$\Theta_{C_2H_4}^{weak,eq}(F_{C_2H_4}) = \frac{F_{C_2H_4} S_{C_2H_4} \Theta_{C_2H_4}^{weak,max}}{F_{C_2H_4} S_{C_2H_4} + k_d \Theta_{C_2H_4}^{weak,max}} \qquad (5)$$

The solid line in Figure 9 is the result of fitting eq 5 to the ethylene data and corresponds to values of $\Theta_{C_2H_4}^{weak,max}$ = 0.03 ML and $k_d/S_{C_2H_4}$ = 0.6 s^{-1}.

3.4. Hydrogenation of Ethylene to Ethane. In this section we address the kinetic aspects of the hydrogenation of ethylene to ethane. Data will be presented for the dependence of the hydrogenation rates on the surface coverages of predosed hydrogen, weakly-adsorbed ethylene, and ethylidyne and on the temperature of the surface.

3.4.1. Effect of Preadsorbed Hydrogen. The effect of predosed hydrogen on the kinetics of ethylene hydrogenation is illustrated in Figure 10, which displays three examples for the time evolution of the ethylene hydrogenation rate (the 30 amu signal) during ethylene dosing at 230 K on Pt(111) surfaces predosed with different amounts of hydrogen. The horizontal solid lines in the top panel mark the level of the background ethane intensity due to impurities in the ethylene beam. It can be seen in this figure that the initial ethane formation rate increases linearly with hydrogen precoverage and also that ethane production requires the direct impinging of ethylene molecules from the beam, because dips are seen in the curves when the ethylene beam is intercepted by the flag. The bottom of Figure 10 displays the trace for the highest H_2 predose (Θ_H^{sat} = 0.5 ML) on a logarithmic scale and confirms that the time evolution of the ethane partial pressure follows an exponential decay, indicating first-order kinetics in hydrogen coverage (see also Figure 11), and that the decay process does stop during the blocking of the beam and resumes upon removal of the flag. This latter effect was observed even when the beam was switched off for 3 min and then restarted again.

Figure 11 summarizes the dependence of the initial rate of ethane formation on the amount of H_2 predosed at T = 230 K. This rate exhibits an increase with hydrogen coverage, as indicated before, in spite of the fact that the overall C_2H_4 uptake

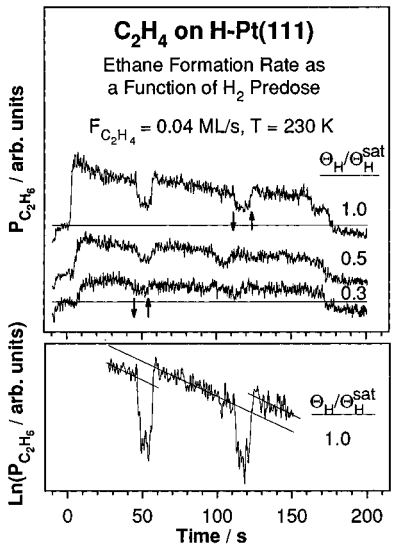

Figure 10. (top) Ethylene partial pressure as a function of time for Pt(111) surfaces first predosed with different amounts of hydrogen and then exposed to a constant ethylene beam ($F_{C_2H_4}$ = 0.04 ML/s) at 230 K. The arrows indicate the points in time when the beam was blocked during the exposure (down arrows) and unblocked again (up arrows). (bottom) Ethane trace for the highest hydrogen predose (Θ_H = 0.5 ML) on a logarithmic scale.

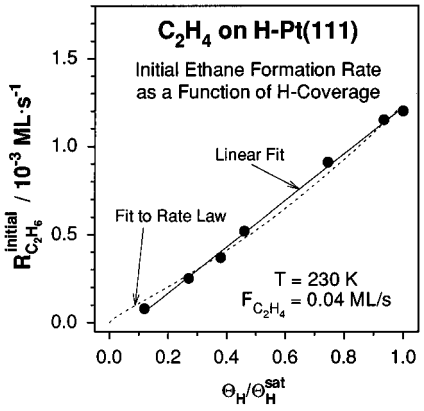

Figure 11. Initial rate for ethane formation ($R_{C_2H_6}^{init}$) as a function of hydrogen predose on a Pt(111) surface exposed to a constant ethylene flux ($F_{C_2H_4}$ = 0.04 ML/s) at 230 K. The solid line is a linear fit to the data points, while the dashed line is the polynomial fit explained in the text.

declines linearly with the amount of predosed H_2 (Figure 6b). The solid line in this figure is a linear fit to the data, while the dashed curve is a polynomial fit that takes into account the slight increase in the amount of weakly-adsorbed ethylene with hydrogen coverage seen in Figure 7 and a dependence of the hydrogenation rate on the weakly-adsorbed ethylene of 1.2, as discussed below. This latter fit yielded a kinetic order of 0.8 ± 0.2 for the hydrogenation rate on the amount of preadsorbed hydrogen.

The mechanistic details on how adsorbed hydrogen participates in the hydrogenation reaction were investigated further by experiments with mixed H_2 + C_2H_4 beams. The H_2:C_2H_4 ratios were varied from 3:1 to 2400:1, but in no case did the observed rate exceeded that obtained for a pure C_2H_4 beam of the same ethylene flux impinging on a hydrogen-predosed Pt(111) surface at the same surface temperature.[25] These results suggest that in the case of the mixed beams hydrogen is adsorbed only on free Pt sites before the surface is saturated with ethylene, and that these H atoms then react in the same way as if hydrogen is preadsorbed. Indeed, when the Pt(111) surface was first saturated with ethylene and then exposed to a pure

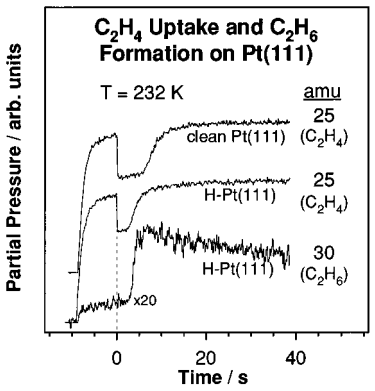

Figure 12. Partial pressures of ethylene (25 amu) and ethane (30 amu) during exposure of clean and hydrogen-predosed ($\Theta_H = 0.5$ ML) Pt-(111) surfaces to a constant ethylene beam ($F_{C_2H_4} = 0.04$ ML/s) at 232 K. The dashed line ($t = 0$ s) marks the point at which the exposure of the surface to the ethylene beam was started.

hydrogen beam, neither ethane formation nor hydrogen adsorption was seen at all. The absence of hydrogen adsorption was also tested by hydrogen TPD experiments after the isothermal exposures, which did not show any additional intensity apart from that due to ethylene decomposition. All this implies that the adsorption of hydrogen competes unfavorably with that of ethylene.

3.4.2. Relevance of Weakly-Adsorbed Ethylene. The effect of the nature of the adsorbed ethylene on ethane formation was inspected next. Figure 12 relates the behavior of the ethylene uptake to the rate of ethane production at 232 K. The two spectra at the top show the time evolution of the ethylene partial pressure (25 amu) during exposures of clean and hydrogen-predosed ($\Theta_H = 0.5$ ML) Pt(111) surfaces to the C_2H_4 beam, respectively, while the third represents the temporal changes in the ethane production rate (30 amu) for the H_2-predosed surface. The figure shows that the production of ethane starts only after the threshold coverage at which the change in ethylene adsorption kinetics is reached, namely, at the point where the adsorption changes from precursor-mediated to Langmuirian (see Figures 5 and 6). At that coverage the rate of the hydrogenation reaction increases steeply, reaches its maximum (at the time when the ethylene adsorption is completed), and follows a slow exponential decay that extends beyond the length of the experiment. This suggests that the two types of ethylene that exist on the surface, namely, the strongly-bound species that adsorbs on the clean surface at low coverage and the weakly-bound state that adsorbs reversibly at saturation, behave differently with regard to ethane formation and that only the latter is involved in the ethane formation seen here. This was further confirmed by experiments like those in Figure 12 but where the ethylene beam was switched off for 2 min, after reaching the threshold coverage where the formation of ethane begins, and then turned on again (data not shown here). The second time the rate of ethane formation was seen to start virtually immediately after turning on the beam, without any time delay. Clearly, only a small amount of additional surface ethylene is needed on the ethylene-saturated substrate in order to restart the hydrogenation process.

The dependence of the initial rate of ethane formation ($R^{init}_{C_2H_6}$) on both ethylene flux ($F_{C_2H_4}$) and weakly-adsorbed ethylene coverage ($\Theta^{weak}_{C_2H_4}$) is shown in Figure 13. It is interesting to notice here the fact that the rates of both ethane formation and ethylene desorption from the weakly-bound state show an approximately similar flux dependence, as seen by comparing the corresponding data in Figures 13 (hollow circles) and 9. The dependence of the initial rate of ethane formation

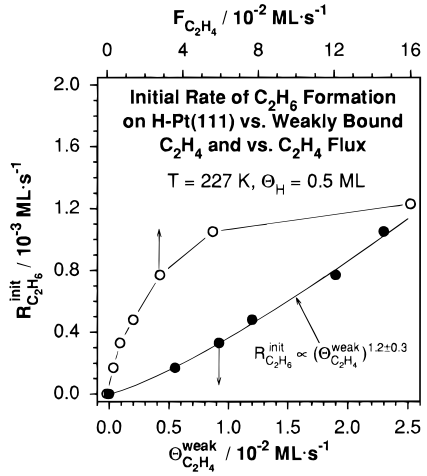

Figure 13. Dependence of the initial rate for ethane formation ($R^{init}_{C_2H_6}$) on both the coverage of weakly-adsorbed ethylene ($\Theta^{weak}_{C_2H_4}$), full circles and bottom scale) and the ethylene flux ($F_{C_2H_4}$, hollow circles and top scale). The solid line through the $R^{init}_{C_2H_6}$ ($\Theta^{weak}_{C_2H_4}$) data points is a polynomial fit corresponding to a kinetic order of 1.2 ± 0.3.

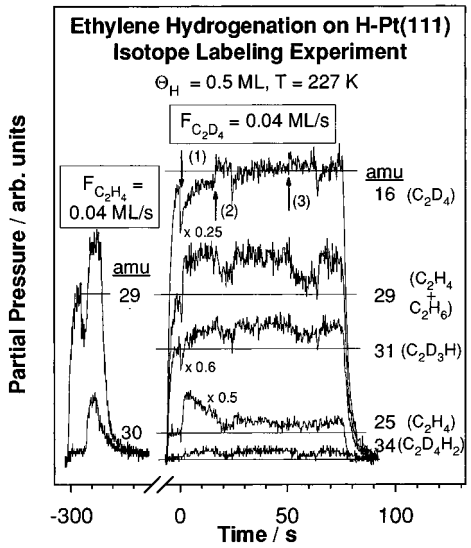

Figure 14. (left) Time evolution of the ethylene (29 amu) and ethane (30 amu) partial pressures during exposure of a hydrogen-predosed ($\Theta_H = 0.5$ ML) Pt(111) surface to a normal ethylene beam ($F_{C_2H_4} = 0.04$ ML/s) at 227 K. (right) Data after the C_2H_4 beam was shut off and the surface was exposed to a constant C_2D_4 beam ($F_{C_2D_4} = 0.04$ ML/s). Shown in this second part of the figure are the partial pressures of the incoming C_2D_4 (16 amu), of the desorbing C_2H_4 (25 and 29 amu), and of some of the reaction products, namely, C_2H_6 (29 amu), C_2D_3H (31 amu), and $C_2D_4H_2$ (34 amu), as a function of dosing time.

on the amount of weakly-adsorbed ethylene (solid circles) was fitted by a polynomial function which revealed a nearly first-order (1.2 ± 0.3) dependence of the first on the second (solid line through $R^{init}_{C_2H_6}$ ($\Theta^{weak}_{C_2H_4}$) data).

Additional information on the role of the weakly-adsorbed ethylene in the hydrogenation process was obtained by kinetic experiments using isotopic labeling. The experimental sequence used here is exemplified by the data in Figure 14: (1) The Pt-(111) surface was initially predosed with H_2 and then exposed to a C_2H_4 beam at 227 K until saturation was reached and the ethane formation rate past its maximum point. The left part of Figure 14 shows the traces for 29 and 30 amu for this first phase of the experiment. Note that the 29 amu signal in this case is mainly due to ethylene but nevertheless displays some additional intensity above the horizontal line from cracking of ethane in the mass spectrometer. (2) The ethylene beam was then blocked

and switched off, a process that resulted in an immediate decay of the ethane signal (as seen in the 30 amu trace; the decay of the 29 amu signal is delayed somewhat since blocking of the beam also leads to ethylene desorption from the surface), and the system was left to rest for 4 min. (3) A C_2D_4 beam was then switched on, and the flag was removed at the point indicated by arrow 1. (4) Finally, the beam was intercepted again for a few seconds at the points indicated by arrows 2 and 3.

In regard to the kinetics for ethylene adsorption during the isotope-labeling experiments, the traces for 16 and 25 amu were chosen in Figure 14 to represent C_2D_4 and C_2H_4, respectively, even though the signals of the complete cracking pattern were recorded during the experiment. The signal for C_2D_4 shows an initial adsorption dip immediately after exposure of the surface to the beam followed by a gradual return to its equilibrium value (horizontal line), which happened within approximately 40 s. The trace for C_2H_4, on the contrary, increases steeply after exposure of the ethylene-saturated surface to the C_2D_4 beam and reaches a maximum value within a few seconds and then decays slowly to its equilibrium value (horizontal line) over the same 40 s period of time. These two opposite results argue for the displacement of some of the adsorbed C_2H_4 by the incoming C_2D_4. A comparison of the amounts of C_2H_4 adsorbed in the first step of the experiment to the amount desorbed after exposing the surface to the C_2D_4 beam reveals that between 80 and 100% of the initial surface C_2H_4 desorbs within the first 40 s of exposure to the C_2D_4 beam.

Next, the traces for 29 and 34 amu were used to monitor the hydrogenation reaction. The signal for mass 34 amu, which corresponds to $C_2D_4H_2$ from hydrogenation of the incoming C_2D_4 with surface H exclusively, barely rises above the background for the first 10 s of exposure of the surface to the C_2D_4 beam but grows slowly afterward until reaching a low steady-state value. The contribution from 29 amu, on the other hand, rises immediately above the background after removing the flag (arrow 1) and reaches almost the same value as in the first half of the experiment with the C_2H_4 beam (see left part of Figure 14). These data suggest that most of the hydrogenation that takes place immediately after removing the flag in the second half of the experiment involves C_2H_4, not C_2D_4, even though the beam contains only deuterated ethylene. It appears therefore as if the ethylene being hydrogenated is that adsorbed in the first half of the experiment, not that arriving from the beam.

Finally, one of the problems with labeling experiments for studying hydrogenation reactions involving C_2D_4 and C_2H_4 on Pt(111) is that the simultaneous H/D exchange processes that occur on the surface lead to a partial scrambling of the deuterium distribution in the isotopically-labeled hydrocarbons.[26,27] To obtain an estimate for the influence of this effect on our kinetic measurements, the signal for 31 amu, which corresponds to the C_2D_3H produced by a single H/D exchange on C_2D_4, is included in Figure 14. It has to be kept in mind that there is a background level in this signal due to the $^{13}CCD_3^+$ from C_2D_4 (marked in the figure by a horizontal line) and that the dip right after removing the flag results from the C_2D_4 adsorption discussed above. Nevertheless, the intensity of the 31 amu signal does increase above the background level after longer C_2D_4 exposures and decreases when intercepting the beam with the flag (arrow 2) despite the increase in the C_2D_4 background (16 amu, top spectrum). This means that H−D scrambling products do indeed desorb from the surface. However, judging from the magnitude of the change in the 31 amu trace in Figure 14, this H/D exchange can be considered reasonably small in these experiments, at least during the first 5−10 s of exposure of the surface to the C_2D_4 beam.

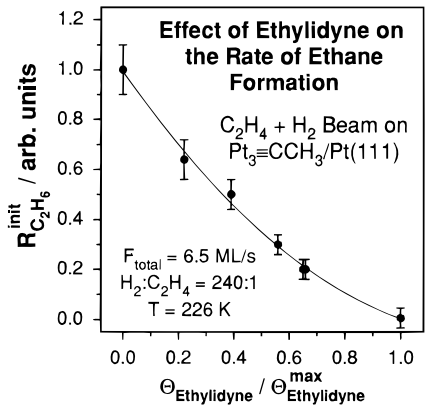

Figure 15. Initial reaction rates for ethane formation on Pt(111) as a function of ethylidyne ($Pt_3{\equiv}CCH_3$) precoverage when exposed to a mixed $H_2 + C_2H_4$ beam with $H_2:C_2H_4 = 240:1$ at 226 K. Total beam flux: $F = 6.5$ ML/s.

3.4.3. Effect of Coadsorbed Ethylidyne. The effect that chemisorbed ethylidyne has on the hydrogenation chemistry of ethylene was characterized by experiments on Pt(111) surfaces precovered with various amounts of ethylidyne, which was deposited by dosing submonolayer coverages of ethylene at 200 K and heating to 350 K for approximately 3 min. The ethylidyne coverages were calibrated by measuring the H_2 desorption signal during heating and ratioing that against the signal from a saturation layer, $\Theta^{max}_{ethylidyne}$, which was taken to correspond to 0.25 ML.[12,13] Figure 15 displays the resulting initial ethane formation rates ($R^{init}_{C_2H_6}$) at 226 K as a function of ethylidyne coverage obtained by using a $H_2 + C_2H_4$ mixed beam with a $H_2:C_2H_4 = 240:1$ ratio in order to maximize the hydrogenation yield. The data were fitted to a second-order polynomial (solid line), but a linear relationship between ethylidyne coverage and hydrogenation rate would still be in reasonable agreement with the experimental results. The monotonic decrease in hydrogenation rate with ethylidyne precoverage implies that the presence of ethylidyne on the surface does not influence the hydrogenation reaction in any significant way other than by blocking adsorption sites, at least under the conditions of these experiments. The hydrogenation of ethylene over an ethylidyne-saturated layer, if it occurs, has a rate below the detection limit of our technique.

3.4.5. Temperature Dependence. Lastly, the temperature dependence of the hydrogenation rate for the weakly-adsorbed ethylene to ethane was measured by exposing H_2-predosed Pt(111) surfaces to a constant ethylene beam at different surface temperatures. Test hydrogen TPD experiments were used to confirm that the H_2 predoses lead to the same hydrogen coverage (approximately 0.5 ML) for all surface temperatures included in Figure 16, and high C_2H_4 fluxes (0.3 ML/s) were used to ensure that the concentration of weakly-bound ethylene was also set to the same near-saturation value for the whole temperature range. The data obtained in this study, displayed in an Arrhenius plot in Figure 16, yielded an activation energy value of $E_a = 6 \pm 1$ kcal/mol.

3.5. Temperature-Programmed Desorption Experiments. Finally, the conclusions from the isothermal kinetic experiments presented above were tested with temperature-programmed desorption (TPD) experiments. Figure 17 shows a compilation of ethylene (27 amu, a), hydrogen (2 amu, b), and ethane (30 amu, c) TPD spectra from Pt(111) surfaces predosed with a constant amount of H_2 ($\Theta_H = 0.5$ ML) and then exposed to an ethylene beam ($F_{C_2H_4} = 0.04$ ML/s) for approximately 180 s at

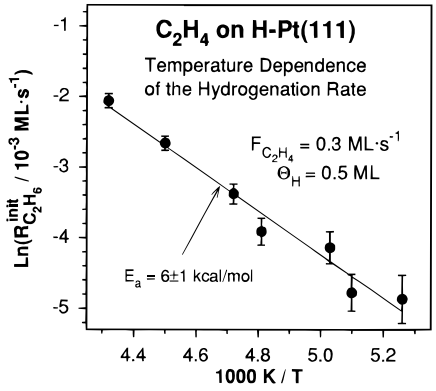

Figure 16. Arrhenius plot for the initial rate of ethane formation ($R^{init}_{C_2H_6}$) on hydrogen-precovered (Θ_H = 0.5 ML) Pt(111) surfaces exposed to a constant ethylene beam ($F_{C_2H_4}$ = 0.3 ML/s).

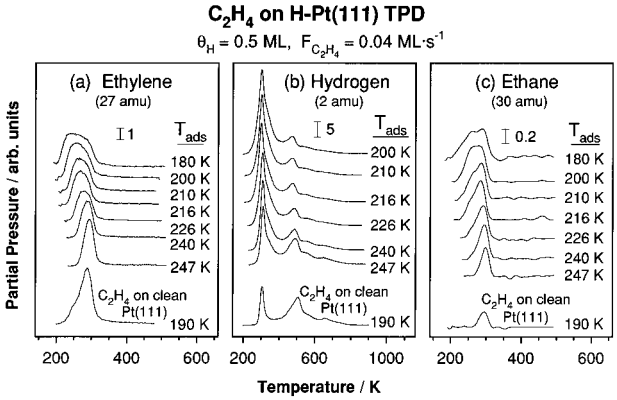

Figure 17. Ethylene (a, left), hydrogen (b, center), and ethane (c, right) temperature-programmed desorption (TPD) spectra from hydrogen-predosed (Θ_H = 0.5 ML) Pt(111) surfaces after saturation with C_2H_4 at the indicated temperatures ($F_{C_2H_4}$ = 0.04 ML/s, 180 s exposure time). The bottom trace in each panel corresponds to the TPD from a clean Pt(111) surface saturated with ethylene at 200 K.

different surface temperatures (as indicated in the figure). The bottom and top traces in each panel correspond to the TPD from clean and hydrogen-predosed Pt(111) surfaces saturated with ethylene at low temperature (180−200 K), respectively. Ethylene desorption from the clean Pt(111) surface mostly originates from a strongly-bound state at 285 K; only a minor fraction desorbs at lower temperatures. (There is a shoulder in the TPD signal at about 245 K.) The presence of hydrogen on the surface, on the other hand, results in an obvious increase in the population of weakly-bound ethylene (Figure 17a). In addition, increasing the surface temperature during dosing from 180 to 247 K gradually transforms the ethylene TPD signal toward that for ethylene on clean Pt(111): the intensity of the weakly-bound ethylene seen in the TPD declines while that of the strongly-bound ethylene increases.

The H_2 TPD traces for the same experiments, shown in Figure 17b, display a sharp low-temperature desorption peak ascribed to the desorption of both the preadsorbed hydrogen and that produced by the conversion of ethylene into ethylidyne and a broad feature above 400 K due to the decomposition of ethylidyne.[3] The ratio of the areas under these two peaks for the case of ethylene dosed on a Pt(111) surface with no preadsorbed hydrogen is 1:3, as expected from stoichiometric considerations, but it is much larger in the other cases because of the contribution from the predosed H_2. The H_2 TPD spectra from ethylene dosed on hydrogen-precovered surfaces also consists of two main features at approximately 300 and 475 K, and although the small peak at 475 K is about 30 K lower than the broad ethylidyne decomposition peak at 505 K (bottom

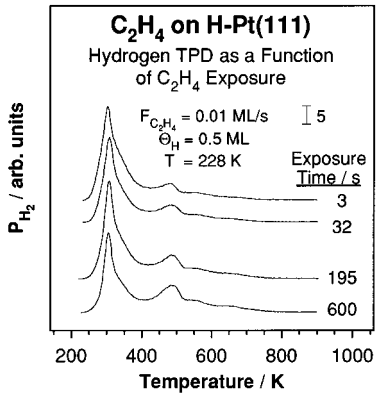

Figure 18. Hydrogen TPD from a Pt(111) surface predosed with hydrogen (Θ_H = 0.5 ML) and then exposed to a constant ethylene beam ($F_{C_2H_4}$ = 0.01 ML/s) at a surface temperature of 228 K for different periods of time.

spectrum), it is also likely to be associated with ethylidyne decomposition. The peak around 300 K, however, is now much broader than in the ethylene reference spectrum and is mostly due to the preadsorbed hydrogen. Again, increasing the dosing temperature in the case of the hydrogen-predosed surfaces leads to spectra similar to those from the clean Pt(111).

The general trend as a function of adsorption temperature seen in the ethane TPD shown in Figure 17c is similar to that found for ethylene desorption (Figure 17a). In the case of ethylene adsorption on H_2-predosed surfaces at 180 K, the partial pressure of ethane rises at approximately 200 K and yields a broad TPD peak which extends to about 300 K, but dosing at higher surface temperatures reduces the low temperature part of the peak and eventually leads to a spectrum similar to that for the bare Pt(111) surface. The changes in the shape of this desorption feature are also accompanied by a decrease in the overall hydrogenation yield, by about a factor of 5, a result that is in qualitative agreement with the findings of other investigations.[28]

Finally, Figure 18 reflects the changes in the chemical behavior of the H_2-predosed Pt(111) surfaces induced by the time they are exposed to the ethylene beam. Shown are hydrogen (2 amu) TPD traces for several beam exposure times after ethylene saturation. In the case of waiting only 3 s after reaching saturation (top spectrum), the TPD displays a broad feature around 300 K and a small peak around 480 K, as shown before, and the ratio of hydrogen that desorbs below and above 400 K is approximately 2.5:1. As discussed above, this ratio is approximately 1:3 when hydrogen originates exclusively from the formation and decomposition of ethylidyne, and it is high here because most of the hydrogen desorption in the 300 K peak comes from the hydrogen adsorbed on the surface before ethylene exposure. After longer exposure times to the ethylene beam, however, the ratio of the hydrogen that desorbs below and above 400 K decreases, to 1.1:1 for the 600 s trace. Also, the absolute yield for hydrogen desorption above 400 K increases with ethylene exposure, indicating that more ethylene adsorbs on the surface over time. These results imply that ethylene either displaces or reacts slowly with surface hydrogen and that this opens up new sites for ethylene adsorption.

4. Discussion

The isothermal experiments described above have allowed for the separation of the kinetics of each of the reactions involved in the thermal conversion of ethylene on Pt(111) around room temperature, namely, molecular adsorption−desorption, ethylidyne formation, and hydrogenation to ethane.

In the subsequent sections each process will be discussed in more detail. For that, the following general mechanism will be used:

$$C_2H_4(g) \underset{k_b}{\overset{k_f}{\rightleftharpoons}} C_2H_4(ad) \quad (6)$$

$$C_2H_4(ad) \xrightarrow{k_1} Pt_3{\equiv}CCH_3(ad) + H(ad) \quad (7)$$

$$C_2H_4(ad) + H(ad) \underset{k_{-2}}{\overset{k_2}{\rightleftharpoons}} Pt_n{-}C_2H_5(ad) \xrightarrow{+\,H\ (fast)} C_2H_6(g) \quad (8)$$

$$2H(ad) \underset{k_{-3}}{\overset{k_3}{\rightleftharpoons}} H_2(g) \quad (9)$$

Here eq 6 takes into account the adsorption−desorption kinetics of ethylene on Pt(111) surfaces, eq 7 describes the formation of ethylidyne, eq 8 describes the stepwise hydrogenation of ethylene with surface H to ethane, and eq 9 describes the adsorption−desorption kinetics of hydrogen. In addition, two types of adsorbed ethylene need to be considered in the overall scheme: a strongly-bound species that forms at low coverages, and a weakly-bound state that is produced at high ethylene coverages or in the case of coadsorption with hydrogen.

4.1. Adsorption of Ethylene on Clean and H_2-Predosed Pt(111). The chemisorption of ethylene on Pt(111) surfaces has been studied extensively in the past. Adsorption at low temperatures results in a weakly π-bonded ethylene species which can rehybridize to di-σ bonded ethylene above 52 K.[29−31] It has also been reported recently that a certain population of π-bonded ethylene molecules can be maintained on Pt(111) at higher temperatures under high ethylene pressures.[23,24] The presence of either alkali or oxygen atoms on the Pt(111) surface can similarly lead to a weaker π ethylene−metal interaction at temperatures above 130 K.[30,32] LEED investigations indicate that the di-σ-bonded ethylene molecules occupy 3-fold hollow sites (with a higher occupation probability for fcc 3-fold hollow sites) of the surface.[33] Finally, the surface saturation coverage of ethylene has been the source of some controversy, since a few reports have argued for a coverage of 0.50 ML,[34,35] but most of the published work agrees on a value of 0.25 ML instead;[12−14,36−38] this latter value was used here to calibrate the ethylene flux of our doser.

The sticking coefficient versus coverage data for ethylene on Pt(111) shown in Figure 6a reveal that, at least at low temperatures, the type of adsorption changes from non-Langmuirian to Langmuirian at coverages near saturation. Ethylene TPD data as a function of ethylene coverage indeed show a low-temperature shoulder at approximately 245 K for the near-saturation coverages where the Langmuirian adsorption takes place (Figure 17a, bottom spectrum). In addition, blocking of the beam to the surface after reaching the end of the ethylene uptake leads to the reversible desorption of some of the surface ethylene, as illustrated by the kinetic data in Figure 7. From these observations it can be speculated that either at low temperatures or in the presence of an ethylene flux the surface coverage can be increased past the 0.25 ML mark to produce an ethylene layer in which lateral molecular interactions lead to a reduced desorption temperature. It is tempting to associate the strongly-bound species that forms at low coverages with a di-σ-type bonding and the weak state seen at saturation with a π ethylene−metal interaction. It is also possible that the transition from strongly- to weakly-bound ethylene may not be the effect of sequential filling of different adsorption states. This is suggested by the observation that 80% or more of the normal C_2H_4 initially adsorbed on the surface can be displaced by C_2D_4 molecules when exposing this surface to a C_2D_4 beam, a behavior that could be explained by assuming that the increase in coverage leads to the formation of a more densely packed layer in which all molecules become equivalent but more loosely bound to the surface. Alternatively, there could be a facile exchange between the strongly σ-bound molecules on the surface and those weakly-bound in a precursor state which becomes populated by molecules arriving from the gas phase. Regardless of which explanation is correct, these observations are important for the understanding of ethylene hydrogenation, because even though it seems that only the weakly-bound molecules hydrogenate under the reaction conditions used here, a large amount of the normal C_2H_4 dosed initially is hydrogenated first in the isotope labeling experiments (Figure 14). This point will be discussed in more detail below.

It was also shown in this paper that hydrogen preadsorption changes the adsorption characteristics of ethylene. The adsorption of H_2 on Pt(111) is known to be dissociative, with the H atoms occupying 3-fold hcp hollow sites up to saturation, which corresponds to a coverage of 1 ML.[39−41] The hydrogen TPD spectra from hydrogen-dosed Pt(111) surfaces show a rather complicated behavior, with two distinctive desorption maxima above 200 K which have been explained by lateral interactions among the H atoms.[22] In our study the hydrogen coverages were kept below 0.5 ML, a regime where the hydrogen TPD displays only one high-temperature desorption peak. Since the interaction between H atoms on the Pt(111) surface is repulsive (the heat of adsorption decreases with increasing coverage[40]), it can be assumed that the hydrogen atoms at these low coverages are uniformly spread over the surface.

Given that both ethylene and hydrogen occupy 3-fold hollow sites on the clean Pt(111) surface, a competition for adsorption sites between the two species is to be expected. Indeed, the total amount of adsorbed C_2H_4 at saturation decreases linearly with H precoverage, as illustrated in Figure 6b. The specific manner in which this happens is highlighted in Figure 6a, which shows that hydrogen mainly reduces the uptake of the C_2H_4 molecules that adsorb during the initial precursor-mediated period (reduction by a factor of 3.3 in going from clean Pt(111) to $\Theta_H = 0.5$ ML), and that the number of molecules adsorbed during the Langmuirian adsorption is reduced to a much lesser extent (reduction by a factor of 1.5 in the same experiment). As a consequence of this, the ratio of ethylene adsorbed in the precursor-mediated regime to that added in the Langmuirian regime decreases from approximately 2:1 to 1:1 as the hydrogen precoverage is increased from $\Theta_H = 0$ ML to $\Theta_H = 0.5$ ML.

Hydrogen predosing also leads to an absolute increase in the amount of reversibly adsorbed ethylene, as illustrated by the results of Figure 7: for the same ethylene flux ($F_{C_2H_4} = 0.04$ ML/s) and surface temperature (232 K), blocking of the ethylene beam in the case of the H_2-predosed surface leads to a higher rate of C_2H_4 desorption (by a factor of 2) compared to that on the clean Pt(111) surface (although the total amount of adsorbed ethylene decreases by a factor of about 3). In addition, the ethylene TPD spectra display a markedly higher ethylene desorption rate from the H_2-predosed surfaces at temperatures below 250 K (Figure 17a and ref 42). Also, the kinetic data presented in Figure 8 and the TPD data in Figure 17a show that the weakly-adsorbed ethylene species is stable on the hydrogen-predosed Pt(111) surfaces at temperatures below approximately 200 K. The amount of weakly-adsorbed ethylene that can be maintained on a H_2-predosed Pt(111) surface increases in a Langmuirian fashion as a function of the ethylene flux in front of the surface (Figure 9) and at 227 K reaches a

maximum coverage of 0.03 ML, which corresponds to about one-third of the total ethylene coverage under the conditions of the experiment. The desorption rate constant for this case is assumed to be independent of the surface coverage, as justified by the fact that at high coverages the ethylene uptake data (the sticking coefficient as function of coverage in Figure 6a) can be described this way within the accuracy of the experiment. Finally, the desorption of ethylene after blocking the beam to the surface follows the exponential decay characteristic of simple first-order kinetics.

4.2. Ethylidyne Formation. At surface temperatures above approximately 240 K, ethylene is known to form ethylidyne ($Pt_3{\equiv}CCH_3$) on the Pt(111) surface. The mechanism for ethylidyne formation has been extensively studied by many techniques, including HREELS,[41,43] TPD,[28,44] STM,[45] LEED,[46] SFG,[47] laser-induced desorption (LID),[19] and infrared spectroscopy,[16,26] but it is still not fully understood. The experiments undertaken in this study have provided a new experimental approach to measuring the kinetics of this reaction based on monitoring the desorption of the resulting hydrogen from the Pt(111) surface. In order to estimate the activation energy for the formation of ethylidyne from the hydrogen desorption data (Figures 2 and 3), the following assumptions and approximations have been applied to the mechanism given above:

(1) Since the C_2H_4 uptake data indicate that the desorption of H_2 from ethylene decomposition starts only at coverages close to saturation (Figure 1), it was assumed that at $T = 220$ K the net ethylidyne formation rate (eq 7) was essentially uninfluenced by the kinetics of the ethylene adsorption.

(2) The hydrogenation process, eq 8, was neglected. This was justified by the experimental finding that less than 10% of the ethylene molecules react to ethane under the conditions described in Figure 2, as discussed in the text (see Figure 4).

(3) The hydrogen desorption process was assumed to be reaction limited, which means that no accumulation of H atoms takes place on the surface (i.e., the coverage of surface hydrogen reaches a low steady-state value soon after the conversion of ethylene is initiated).

Following these assumptions, the rate for the formation of ethylidyne can be calculated from the measured hydrogen desorption data by using a simple first-order rate equation:

$$\frac{d\Theta_{Pt_3{\equiv}CCH_3}}{dt} = 2\frac{d\Theta^{gas}_{H_2}}{dt} = -\frac{d\Theta_{C_2H_4}}{dt} = k_1\Theta_{C_2H_4} \qquad (10)$$

The inset in Figure 3 shows an Arrhenius plot for the values of k_1 obtained by applying eq 10 to the decay data in Figure 2 down to 25% of the starting value. The resulting activation energy, $E_a = 15 \pm 2$ kcal/mol, is in reasonable agreement with values obtained by other experimental methods (17 kcal/mol by TPD,[28] 15 kcal/mol by SIMS,[17] 14.4 kcal/mol by NEXAFS,[18] 18.4 kcal/mol by LID and IR[19]). Furthermore, LID experiments have indicated that there is a change in the rate of disappearance of ethylene from the surface once a major part of the surface has been converted to ethylidyne,[19] but that the rate of ethylidyne formation follows first-order kinetics over the whole coverage range probed. This is also in agreement with the linear nature of the data shown in Figure 3.

4.3. Ethylene Hydrogenation to Ethane. At high temperatures (above 240 K) some ethane formation is seen even on surfaces dosed with ethylene alone. This ethylene self-hydrogenation process has been previously studied by TPD.[7,28] It has been shown that the decomposition of ethylene to ethylidyne is the only significant source of surface H for that hydrogenation reaction. In order to understand the kinetics of this self-hydrogenation, therefore, it is important to note that the decay of the C_2H_4 concentration on the surface over time is approximately proportional to the decay of the signal of the hydrogen that evolves into the gas phase. Since the time evolution of the hydrogen (which is proportional to the coverage of ethylene) and ethane signals follow each other closely, the decrease in C_2H_4 concentration on the surface alone could explain the time dependence of the ethane intensity; the hydrogen coverage is likely to reach a small steady-state value early in the conversion process and to be of minor importance for the overall kinetics of the hydrogenation reaction. STM measurements of the ethylidyne formation process suggested that ethylidyne grows in islands on ethylene-saturated Pt(111) surfaces.[45] It can be speculated that the rate of ethylene hydrogenation may be limited by the diffusion of H from the ethylidyne island boundaries into the ethylene layer.[27] This would also be compatible with the fact that the ethane production rate maximum grows at a much slower pace than the maximum of the H signal with increasing surface temperatures (Figures 2 and 4).

A more detailed study of the kinetics of the ethylene hydrogenation was performed by using hydrogen-precovered Pt(111) surfaces at temperatures below 240 K in order to avoid any effects that changes in either hydrogen coverage or ethylidyne formation rate may have on the overall kinetics for ethane formation. It appears that in this case weakly-bound C_2H_4 molecules play a particularly important role in the hydrogenation reaction, as indicated by the following experimental findings of this investigation:

(1) The time evolution of the ethane signal during exposure of the surface to the ethylene beam does not increase above the background level until the C_2H_4 adsorption changes to Langmuir adsorption, a point associated with the stage at which the weakly-bound ethylene state starts to be populated (Figure 12).

(2) Blocking the ethylene beam, which induces the depopulation of the weakly-bound species, results in an immediate drop in the ethane rate (Figures 1, 4, and 10).

(3) The rate of ethane formation shows a nearly first-order dependence on the amount of weakly-bound ethylene (Figure 13).

Additional information on the role of the weakly-bound ethylene in the hydrogenation process was gained by the results of the isotopic labeling experiments displayed in Figure 14. The desorption of C_2H_4 (25 amu) and the adsorption of C_2D_4 (16 amu) will be addressed first. As already mentioned above (section 4.1), when a Pt(111) surface covered with C_2H_4 is exposed to a C_2D_4 beam, an exchange of C_2H_4 by C_2D_4 takes place until the surface is covered with C_2D_4 only. The same process was also observed on the hydrogen-predosed Pt(111) surfaces first exposed to C_2H_4 and then to C_2D_4, only that in that case the exchange rate immediately after exposing the $C_2H_4/H_2/Pt(111)$ surface to the C_2D_4 beam was approximately 2 times faster for the same surface temperature. Apparently, both C_2D_4 molecules and surface H are involved in the increase in the desorption rate of the ethylene molecules. A more detailed description of this complex interaction, however, requires further investigations. A similar effect of increasing desorption of one surface species induced by the adsorption of a second species has been reported for the coadsorption of CO and hydrogen on Ni as well as for other systems.[48,49]

More insight into the hydrogenation mechanism is provided by the time evolution of two of the possible hydrogenation products during the isotope labeling experiments shown in Figure 14, namely, $C_2D_4H_2$ and C_2H_6. It can be seen there that during the first 5−10 s of exposure to the C_2D_4 beam the rate

of normal ethane formation ($R_{C_2H_6}$, 29 amu) on an ethylene + hydrogen saturated Pt(111) surface reaches about 75% of the original value seen when the predosed surface is exposed to a C_2H_4 beam. The signal for $C_2D_4H_2$ (34 amu), on the other hand, hardly rises above the background during the same period of time. This means that the hydrogenation that takes place on the surface involves all of the adsorbed ethylene molecules, even though it only happens at the high coverages needed to induce the switch in ethylene adsorption to the weak state: at the beginning of the exposure of the surface saturated with C_2H_4 to the C_2D_4 beam most of the ethane produced is of the normal C_2H_6 type (the product of hydrogenation of normal C_2H_4), and yet the C_2D_4 beam is still required to keep a high overall coverage.

Recent studies addressing the hydrogenation of ethylene over Pt(111) under UHV conditions have proposed a model where the formation of an ethyl intermediate is the rate-determining step, but the activation energy for this ethyl formation was estimated to be about 13 kcal/mol,[7] whereas our isothermal kinetic data yielded a value of 6 ± 1 kcal/mol for the complete hydrogenation of ethylene to ethane. This difference in activation energy might reflect the difference in bonding and the resulting difference in hydrogenation chemistry of the weakly-bound ethylene on the H-precovered Pt(111) surface as compared to a situation where the Pt(111) surface is predominantly covered with ethylene;[7] it is the former situation (the one studied here) the closest to real catalytic conditions.

Surface hydrogen also plays a key role in the ethylene hydrogenation reaction. The fact that this hydrogenation requires surface hydrogen is clearly proven by the results from experiments where the Pt(111) surface was predosed with hydrogen and then exposed to a C_2D_4 beam, in which case $C_2D_4H_2$ was practically the only hydrogenation product detected. In order to determine the kinetic order of the reaction in H coverage, the initial hydrogenation rate was also measured as a function of H_2 predose (Figure 11). The analysis of these data requires the inclusion of the changes in the amount of weakly-adsorbed ethylene with hydrogen coverage seen in Figure 7, which is estimated to be about a factor of 2 in going from a pure ethylene surface to a H precoverage of 0.5 ML and to be linear for H coverages in between (data not shown). Using a kinetic order for the hydrogenation reaction in the weakly-adsorbed ethylene of 1.2, as determined from Figure 13, the data for the initial rate of ethane formation ($R^{init}_{C_2H_6}$) versus relative hydrogen coverage ($\Theta^{rel}_H = \Theta_H/\Theta^{sat}_H$, $\Theta^{sat}_H = 0.5$ ML) was fitted to the following equation:

$$R^{init}_{C_2H_6} = k(\Theta^{rel}_H)^x\,(\Theta^{weak}_{C_2H_4})^{1.2} \propto (\Theta^{rel}_H)^x\,(1+\Theta^{rel}_H)^{1.2} \quad (11)$$

The fit of eq 11 to the data for the rate of hydrogenation, shown as a dashed line in Figure 11, yielded a value of 0.8 ± 0.2 for *x*, the kinetic order in hydrogen surface coverage. This implies that the hydrogenation of weakly-adsorbed ethylene molecules most likely also involves the slow formation of ethyl intermediates (eq 8).

The decay of the ethane formation rate with time offers further evidence for this nearly first-order behavior of the hydrogenation rate of ethylene on hydrogen coverage. As already pointed out in the Results section, the signal decay is proportional to the time the surface is exposed to the ethylene beam (Figure 10). For the top trace in Figure 10 ($\Theta_H = 0.5$ ML), the amount of C_2H_6 produced between the initial exposure of the H_2-predosed Pt(111) surface to the ethylene beam ($t = 0$ s) and the point when the rate of ethane formation decreases to 50% of its maximum value ($t = 160$ s) amounts to about 0.12 ML. The number of H atoms lost from the surface by the hydrogenation process (0.24 ML) is therefore about half the number of atoms present on the surface after the predose (0.5 ± 0.2 ML); the amount of H lost during this period by desorption from the surface was measured to be less than 0.1 ML. In view of the almost linear dependence of the ethane formation rate on the H precoverage (Figure 11), this suggests that the loss of surface H is the main cause for the decay of the hydrogenation rate. More direct proof for this assumption is given in Figure 18, which displays the hydrogen TPD signal for the C_2H_4/H_2/Pt-(111) surface after increasing ethylene beam exposure times. A quantitative evaluation of the H loss from these data is difficult, since by losing surface H the coverage of ethylene increases, and that in turn increases the intensity in the hydrogen TPD signal due to the formation of ethylidyne. It can nevertheless qualitatively be seen that the TPD intensity around 475 K (due to the decomposition of ethylidyne) grows relative to the intensity around 300 K (from both desorption of surface hydrogen and ethylidyne formation): The ratio of the H_2 that desorbs below 400 K to the H_2 that desorbs above 400 K changes from 2.5:1 (3 s trace) to 1.1:1 (600 s trace) and therefore gradually approaches the value for a surface covered only with ethylene (1:3).

Finally, the role of ethylidyne in the hydrogenation process is illustrated in Figure 15. Here the evolution of the ethane formation rate with ethylidyne coverage indicates that this species is just a spectator on the surface which does not significantly influence the hydrogenation process in any way other than by blocking surface sites.

4.4. Relevance of the Kinetic Studies Reported Here to the Catalytic Hydrogenation of Ethylene. On H_2-predosed surfaces, the rate for ethane formation changes linearly with Θ_H. In the ethylene self-hydrogenation process seen when ethylene is adsorbed on clean Pt(111), on the other hand, Θ_H reaches a small steady-state value instead and does not significantly influence the rate of ethane production afterward. The question arises as to how does the hydrogen surface coverage behave under catalytic conditions. Something can be learned in this regard from the experiments with the $H_2 + C_2H_4$ mixed beams reported here. The rate for ethane formation in those cases decreases with beam exposure time in the same way as in the experiments with H_2-predosed surfaces exposed to pure ethylene beams and eventually drops to values below the detection limit. Furthermore, even when high hydrogen-to-ethylene ratios are used (up to 2400:1), the rate for ethane formation never surpasses that of the H_2-predosed case under the same conditions. Lastly, with an ethylene-saturated surface, no postdosing of hydrogen either by itself or using a mixed $H_2 + C_2H_4$ beam can induce the production of any ethane. All this suggests that hydrogen competes unfavorably with ethylene for adsorption sites on the surface and that the steady-state coverage of hydrogen on the surface during the catalytic conditions may be quite low and may therefore control the overall hydrogenation rate.

Using a simple Langmuir model for competitive adsorption between hydrogen and ethylene, the hydrogen equilibrium concentration (Θ_H) on the surface can be calculated as a function of hydrogen (P_{H_2}) and ethylene ($P_{C_2H_4}$) partial pressures by the equation

$$\Theta_H = \frac{K_{H_2}^{1/2} P_{H_2}^{1/2}}{1 + K_{H_2}^{1/2} P_{H_2}^{1/2} + K_{C_2H_4} P_{C_2H_4}} \quad (12)$$

where K_{H_2} and $K_{C_2H_4}$ are the equilibrium constants for adsorp-

tion−desorption of the corresponding species. By using the same model to calculate the ethylene surface concentration, and reaction order values of 0.8 in hydrogen and 1.2 in weakly-bound ethylene, as determined in this investigation, the rate for ethane formation ($R_{C_2H_6}$) comes out to be

$$R_{C_2H_6} = k_2\Theta_H^{0.8}\Theta_{C_2H_4}^{1.2} = k_2\frac{[K_{H_2}{}^{1/2}P_{H_2}{}^{1/2}]^{0.8}[K_{C_2H_4}P_{C_2H_4}]^{1.2}}{[1 + K_{H_2}{}^{1/2}P_{H_2}{}^{1/2} + K_{C_2H_4}P_{C_2H_4}]^2} \quad (13)$$

Assuming for the catalytic case that (1) the surface concentration of ethylidyne stays near saturation and does not change significantly under typical experimental conditions, (2) the ethylene surface concentration also stays near saturation, and (3) the product of the equilibrium constant times the partial pressure for ethylene is much larger than both that for hydrogen and unity, eq 13 can be approximated by eq 14:

$$R_{C_2H_6} = k_2\frac{[K_{H_2}{}^{1/2}P_{H_2}{}^{1/2}]^{0.8}[K_{C_2H_4}P_{C_2H_4}]^{1.2}}{[K_{C_2H_4}P_{C_2H_4}]^2} \propto \frac{P_{H_2}{}^{0.4}}{P_{C_2H_4}{}^{0.8}} \quad (14)$$

Experimental values for the reaction orders under catalytic conditions for the hydrogenation of ethylene in hydrogen and ethylene range from approximately 0.5 to 1.3 and −0.5 to 0, respectively,[2,4,50] close to those in the equation above (0.4 and −0.8).

5. Conclusions

The kinetics for the hydrogenation of ethylene over Pt(111) was studied isothermally and under vacuum. Ethylene adsorption was found to be precursor-mediated at low coverages and Langmuirian near saturation, at which point a certain population of weakly-adsorbed ethylene can be maintained on the surface by exposure to a constant flux of ethylene molecules. The presence of hydrogen on the surface increases the amount of this weakly-adsorbed ethylene, a species that was shown to be essential for the hydrogenation process. The kinetic orders of the hydrogenation reaction were determined to be 1.2 ± 0.3 and 0.8 ± 0.2 with respect to the weakly-adsorbed ethylene and hydrogen surface coverages, respectively, and an activation energy of 6 ± 1 kcal/mol for the hydrogenation of ethylene to ethane was measured under the conditions of these experiments. The presence of ethylidyne does not influence the hydrogenation reaction in any other way than by blocking surface sites. All this helps understand the kinetic behavior of olefin hydrogenation processes under catalytic conditions.

Acknowledgment. Funding for this research was provided by grants from the National Science Foundation (CHE-9530191 and CTS-9525761) and the Department of Energy, Basic Energy Sciences (DE-FG03-94ER14472). H.Ö. also gratefully acknowledges financial support from the Welch Foundation. Finally, we want to thank T.V.W. Janssens for helpful discussions.

References and Notes

(1) Bond, G. C. *Catalysis by Metals*; Academic Press: London, 1962.
(2) Horiuti, J.; Miyahara, K. *Hydrogenation of Ethylene on Metallic Catalysts*; Report NSRDS-NBC No. 13; National Bureau of Standards; Washington, DC, 1968.
(3) Zaera, F. *Langmuir* **1996**, *12*, 88.
(4) Zaera, F.; Somorjai, G. A. *J. Am. Chem. Soc.* **1984**, *106*, 2288.
(5) Wieckowski, A.; Rosasco, S. D.; Salaita, G. N.; Hubbard, A.; Bent, B. E.; Zaera, F.; Godbey, D.; Somorjai, G. A. *J. Am. Chem. Soc.* **1985**, *107*, 5910.
(6) Beebe, T. P., Jr.; Yates, J. T., Jr. *J. Am. Chem. Soc.* **1986**, *108*, 663.
(7) Zaera, F. *J. Phys. Chem.* **1990**, *94*, 5090.
(8) Zaera, F. *J. Phys. Chem.* **1990**, *94*, 8350.
(9) King, D. A.; Wells, M. G. *Surf. Sci.* **1972**, *29*, 454.
(10) Liu, J.; Xu, M.; Nordmeyer, T.; Zaera, F. *J. Phys. Chem.* **1995**, *99*, 6167.
(11) Zaera, F.; Liu, J.; Xu, M. *J. Chem. Phys.*, in press.
(12) Kesmodel, L. L.; Dubois, L. H.; Somorjai, G. A. *Chem. Phys. Lett.* **1978**, *56*, 267.
(13) Davis, S. M.; Zaera, F.; Gordon, B.; Somorjai, G. A. *J. Catal.* **1985**, *92*, 240.
(14) Griffiths, K.; Lennard, W. N.; Mitchell, I. V.; Norton, P. R.; Pirug, G.; Bonzel, H. P. *Surf. Sci.* **1993**, *284*, L389.
(15) *Selected Mass Spectral Data; Thermodynamics Research Center Hydrocarbon Project (Standard)*, TRC, Texas Engineering Experimental Station, The Texas A&M University System, 1983.
(16) Moshin, S. B.; Trenary, M.; Robota, H. J. *Chem. Phys. Lett.* **1989**, *154*, 511.
(17) Ogle, K. M.; Creighton, J. R.; Akhter, S.; White, J. M. *Surf. Sci.* **1986**, *169*, 246.
(18) Zaera, F.; Fischer, D. A.; Carr, R. G.; Kollin, E. B.; Gland, J. L. In *Electrochemical Surface Science: Molecular Phenomena at Electrode Surfaces*; Soriaga, M. P., Ed.; ACS Symposium Series Vol. 378; American Chemical Society: Washington, DC, 1988; pp 131−140.
(19) Erley, W.; Li, Y.; Land, D. P.; Hemminger, J. C. *Surf. Sci.* **1994**, *103*, 177.
(20) Madey, T. E. *Surf. Sci.* **1972**, *33*, 355.
(21) Kisluik, P. *J. Phys. Chem. Solids* **1957**, *3*, 95.
(22) Christmann, K.; Ertl, G.; Pignet, T. *Surf. Sci.* **1976**, *54*, 365.
(23) Kubota, J.; Ichihara, S.; Kondo, J. N.; Domen, K.; Hirose, C. *Langmuir* **1996**, *12*, 1926.
(24) Cremer, P. S.; Su, X.; Shen, Y. R.; Somorjai, G. A. *J. Am. Chem. Soc.* **1996**, *118*, 2942.
(25) Zaera, F.; Janssens, T. V. W.; Öfner, H. *Surf. Sci.*, in press.
(26) Janssens, T. V. W.; Zaera, F. *Surf. Sci.* **1995**, *344*, 77.
(27) Janssens, T. V. W.; Zaera, F.; Stone, D.; Hemminger, J. C. To be published.
(28) Godbey, D.; Zaera, F.; Yates, R.; Somorjai, G. A. *Surf. Sci.* **1986**, *167*, 150.
(29) Hugenschmidt, M. B.; Dolle, P.; Jupille, J.; Cassuto, A. *J. Vac. Sci. Technol. A* **1989**, *7*, 3312.
(30) Cassuto, A.; Mane, M.; Hugenschmidt, M.; Dolle, P.; Jupille, J. *Surf. Sci.* **1990**, *237*, 63.
(31) Cassuto, A.; Mane, M.; Jupille, J. *Surf. Sci.* **1991**, *249*, 8.
(32) Windham, R. G.; Bartram, M. E.; Koel, B. E. *J. Phys. Chem.* **1988**, *92*, 2862.
(33) Döll, R.; Gerken, C. A.; Van Hove, M. A.; Somorjai, G. A. *J. Am. Chem. Soc.*, submitted.
(34) Yu, R.; Gustafsson, T. *Surf. Sci.* **1987**, *182*, L234.
(35) Masson, F.; Sass, C. S.; Grizzi, O.; Rabalais, J. W. *Surf. Sci.* **1989**, *221*, 299.
(36) Davis, S. M.; Zaera, F.; Somorjai, G. A. *J. Catal.* **1982**, *77*, 439.
(37) Abon, M.; Billy, J.; Bertolini, J. C. *Surf. Sci.* **1986**, *171*, L387.
(38) Mitchell, I. V.; Lennard, W. N.; Griffiths, K.; Massuomi, G. R.; Huppertz, J. W. *Surf. Sci.* **1991**, *256*, L598.
(39) Bartra, I. P.; Barker, J. A.; Auerbach, J. D. *J. Vac. Sci. Technol.* **1984**, *2*, 943.
(40) Christmann, K. *Surf. Sci. Rep.* **1988**, *9*, 1.
(41) Baró, A. M.; Ibach, H. *J. Chem. Phys.* **1979**, *71*, 4812.
(42) Berlowitz, P.; Megiris, C.; Butt, J. B.; Kung, H. H. *Langmuir* **1985**, *1*, 206.
(43) Steininger, H.; Ibach, H.; Lehwald, S. *Surf. Sci.* **1982**, *117*, 685.
(44) Zaera, F. *Surf. Sci.* **1989**, *219*, 453.
(45) Land, T. A.; Michely, T.; Behm, R. J.; Hemminger, J. C.; Comsa, G. *J. Chem. Phys.* **1992**, *97*, 6774.
(46) Starke, U.; Barbieri, A.; Materer, N.; Van Hove, M. A.; Somorjai, G. A. *Surf. Sci.* **1993**, *286*, 1.
(47) Cremer, P.; Stanners, C.; Niemantsverdriet, J. W.; Shen, Y. R.; Somorjai, G. *Surf. Sci.* **1995**, *328*, 111.
(48) Gland, J. L.; Fischer, D. A.; Shen, S.; Zaera, F. *J. Am. Chem. Soc.* **1990**, *112*, 5695.
(49) Yamada, T.; Zhai, R. S.; Iwasawa, Y.; Tamaru, K. *Bull. Chem. Soc. Jpn.* **1989**, *62*, 267.
(50) Zaera, F.; Somorjai, G. A. In *Hydrogen Effects in Catalysis: Fundamentals and Practical Applications*; Paál, Z., Menon, P. G., Eds.; Marcel Dekker: New York, 1988; pp 425−447.